PERGAMON

Planetary and Space Science 49 (2001) 1523–1530

Planetary and Space Science

www.elsevier.com/locate/planspasci

Large-scale lobate scarps in the southern hemisphere of Mercury

T.R. Watters[a,*], A.C. Cook[a], M.S. Robinson[b]

[a] *Center for Earth and Planetary Studies, National Air and Space Museum, Smithsonian Institution, Washington, DC 20560-0315, USA*
[b] *Department of Geological Sciences, Northwestern University, Evanston, IL 60208, USA*

Received 3 November 2000; accepted 18 January 2001

Abstract

Utilizing Mariner 10 images of Mercury, we derived a digital elevation model to examine the topography of the large-scale lobate scarps Adventure Rupes, Resolution Rupes, and Discovery Rupes. The thrust faults that formed these landforms occur along a rough arc that extends for over 1000 km. The new topography shows that vertical uplift occurred on the same side of the three structures suggesting that the fault-planes all dip to the concave side of the arc. These data also show that Adventure and Resolution Rupes are topographically continuous, suggesting the two features were formed by a single thrust fault on Mercury. If this is the case, the Adventure–Resolution Rupes thrust fault is comparable in scale to the Discovery Rupes thrust fault. It is generally believed that Mercurian lobate scarps were formed by compressional stresses induced in the crust as the planet's interior cooled and shrank. Global contraction models predict that stresses at the planetary surface are horizontally isotropic (horizontal principal stresses being equal) resulting in randomly distributed thrust faults with no perferred orientations. The location, orientation, and geometry of the Discovery and Adventure–Resolution Rupes thrust faults, may not be randomly distributed. Analysis of the inferred stresses that formed these faults suggests that they were influenced by regional stresses or by mechanical discontinuities in the crust possibly caused by buried impact basins. The new topographic data reveal a broad, roughly circular topographic low interpreted to be an ancient impact basin centered near Schubert crater (43°S, 54°W), not far from an inferred stress center (48°S, 58°W). Thus the Discovery and Adventure–Resolution Rupes thrust faults may have been influenced by mechanical discontinuities in the Mercurian crust introduced by ancient buried impact basins. © 2001 Published by Elsevier Science Ltd.

1. Introduction

One of the remarkable characteristics of Mercury imaged by Mariner 10 is the presence of hundreds of landforms described as lobate scarps (Strom et al., 1975). These features occur in linear or arcuate segments, and vary in length from tens to hundreds of kilometers (Strom et al., 1975; Cordell and Strom, 1977). In cross-section, lobate scarps generally consist of two morphologic features, a steeply sloping scarp face and a gently sloping back scarp. In some rare cases, this scarp morphology transitions to a ridge (Strom et al., 1975). The maximum relief of the observed lobate scarps varies from hundreds to over a thousand meters (Watters et al., 1998). Many lobate scarps transect impact craters, and the trace of the scarp through a crater is characterized by offsets in the crater wall and floor materials. This coupled with their cross-sectional morphology is the basis for the interpretation that lobate scarps are the surface expression of thrust faults (Strom et al., 1975; Cordell and Strom, 1977; Melosh and McKinnon, 1988; Watters et al., 1998). A simple kinematic model for the formation of lobate scarps involves deformation of near-surface crustal material over a buried thrust fault that propagates upward and eventually breaks the surface (Watters et al., 1998, 2000). Analysis of the displacement–length relationship of thrust faults associated with Mercurian lobate scarps indicates that the ratio γ of maximum displacement D to fault length L is $6.5\pm3.2\times10^{-3}$ (for a population of lobate scarps $n=10$) using estimates of D based on fault-plane dips $\theta=25^{\circ}$ (the uncertainty is the standard deviation of γ for these faults determined for $\theta=28^{\circ}$, the average of the assumed range of $\theta=20^{\circ}$–35°) (Watters et al., 2000). The value of γ for Mercurian thrust faults is consistent with γ for terrestrial fault populations (Cowie and Scholz, 1992) and Martian thrust faults (Watters and Robinson, 1999; Watters et al., 2000).

The distribution and orientation of thrust faults on Mercury is important in constraining models for the origin of the compressional stresses that formed these structures. Mercurian lobate scarps have a generally uniform distribution, occurring in most of the mapped geologic units (Strom et al., 1975); however, there are fewer scarps in the southern hemisphere between 10°S and 30°S (Cordell

* Corresponding author. Tel.: +1-202-357-1425; fax: +1-202-786-2566.
E-mail address: twatters@nasm.si.edu (T.R. Watters).

0032-0633/01/$ - see front matter © 2001 Published by Elsevier Science Ltd.
PII: S0032-0633(01)00090-3

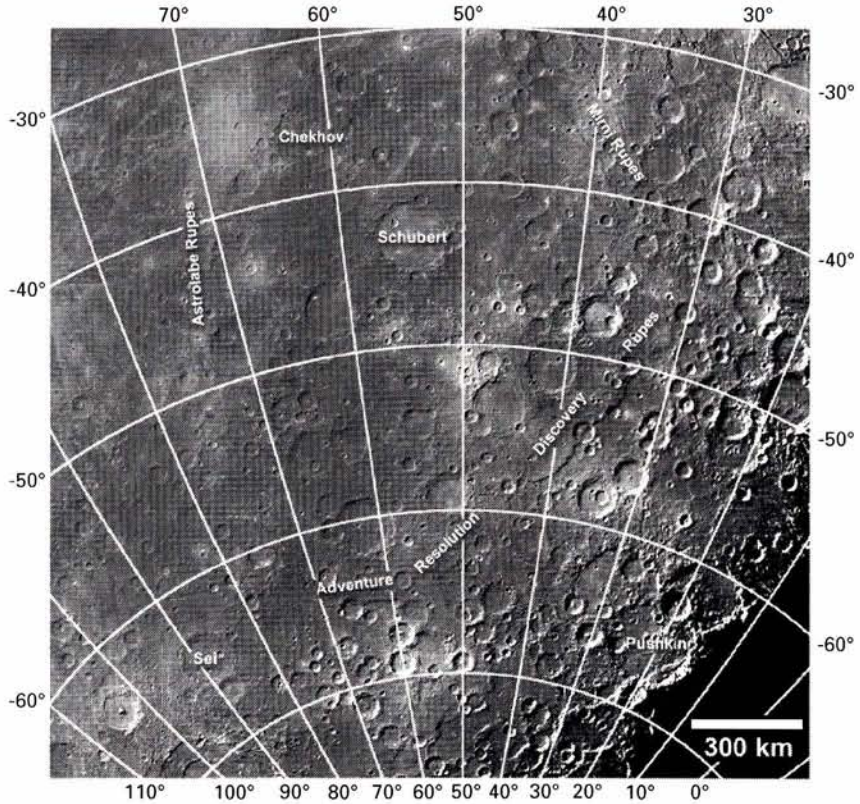

Fig. 1. Mariner 10 mosaic of the Discovery quadrangle area in the southern hemisphere of Mercury. Adventure, Resolution, and Discovery Rupes and other lobate scarps and prominent impact craters are identified.

and Strom, 1977). This local paucity of lobate scarps is consistent with an analysis of compressional strain measured between 70°N and 70°S and 10°W–90°W that showed the least amount of strain was in the equatorial region (20°S–20°N) (Watters et al., 1998). Orientations of the lobate scarps have been the subject of some debate. Cordell and Strom (1977) reported no statistically significant preferred orientation. A N–S preferred orientation was proposed by Melosh and Dzurisin (1978); however, Cordell and Strom (1977) argue that any apparent preferred orientations are due to observational effects. Additionally, using stereocoverage of some areas in the southern hemisphere to reduce any observational bias, Thomas et al. (1988) concluded that lobate scarps have a preferred orientation that is radial to the Caloris basin.

We present the results of a stereoanalysis of a group of three large-scale lobate scarps in the southern hemisphere of Mercury; Adventure, Resolution, and Discovery Rupes (Figs. 1 and 2). An analysis of the orientation, geometry, and inferred stresses is made in an effort to determine if the formation of the thrust faults was influenced by either regional stresses or preexisting mechanical discontinuities in the Mercurian crust.

2. Results

2.1. Topography

In the past, topographic data for Mercury have been obtained from Mariner 10 images and Earth-based radar. The limitation of Earth-based radar altimetry is that it covers only a band $\pm 12^{\circ}$ of the equator (Harmon et al., 1986; Harmon and Campbell, 1988) and the resolution cell is 0.15° longitude $\times 2.5^{\circ}$ latitude or 6 km $\times$ 100 km (Harmon et al., 1986). Elevation data obtained from Mariner 10 images have been derived from shadow measurements (Strom et al., 1975; Malin and Dzurisin, 1976; Pike, 1988), photoclinometry (Hapke et al., 1975; Mouginis-Mark and Wilson, 1981; Schenk and Melosh, 1994; Watters et al., 1998), and point stereoanalysis (Dzurisin, 1978). New topographic data for Mercury are being derived from digital stereoanalysis (Watters et al., 1998; Cook and Robinson, 2000) using updated Mariner 10 camera orientations (Robinson et al., 1999) and improved radiometry (Robinson and Lucey, 1997). Typically, digital stereoanalysis involves manually picking a few tie points to act as starting points for the automated stereomatching process which subsequently finds corresponding points between images using a correlation patch (cf. Day et al., 1992; Thornhill et al., 1993). The image pair

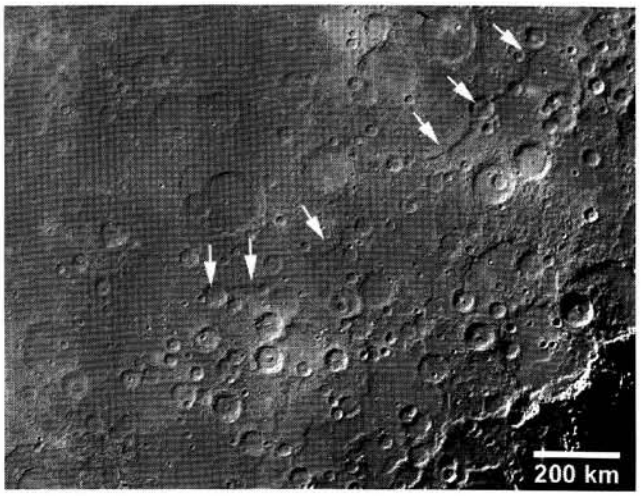

(a)

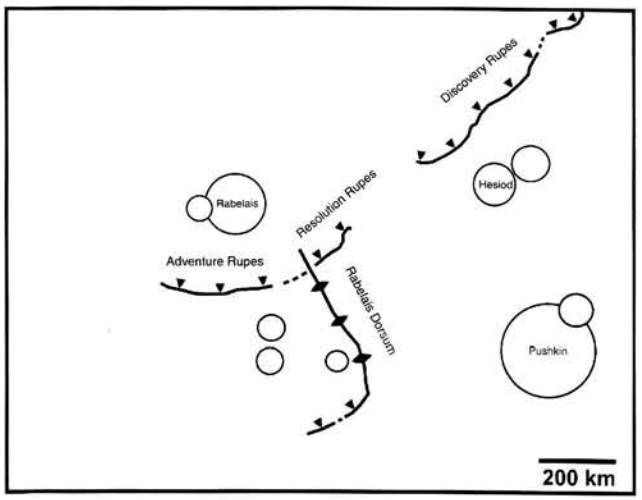

(b)

Fig. 2. (a) Mariner 10 mosaic of the Discovery Rupes region of Mercury showing the location of the Discovery, Resolution, and Adventure Rupes thrust faults (white arrows). (b) Sketch map of the Discovery Rupes region of Mercury identifying the prominent tectonic landforms discussed in the paper (same area shown in (a)).

coordinates found by the matcher are then fed through a stereointersection camera model and the closest point of intersection specifies the location and elevation of the corresponding ground points.

Cook and Robinson (2000) have identified over 2000 Mariner 10 images suitable for stereoanalysis, estimating that approximately 24% of the planet can be topographically mapped to better than ± 1 km theoretical height accuracy and 6% of the surface can be mapped to better than ± 400 m height. The best regional stereoheight accuracy coverage is in the area of the Discovery quadrangle (see Cook and Robinson, 2000; Fig. 1). Within this area are some of the most prominent lobate scarps imaged by Mariner 10, particularly Discovery, Resolution, and Adventure Rupes. We have generated the first regional-scale digital elevation model (DEM) of an area in the Discovery quadrangle using digital stereoanalysis (Fig. 3). The DEM is a composite of elevation data from over 350 individual stereopairs, and has a grid spacing of 2 km/pixel. The theoretical height accuracy of the topographic data varies from ± 1000 m to better than ± 400 m.

2.2. Observations

One of the most striking characteristics of the three lobate scarps, Discovery, Resolution, and Adventure Rupes, is that they occur along a rough arc that extends for over 1000 km (Figs. 1 and 2). The topographic data indicate that Discovery Rupes has the greatest relief ($\sim$1.5 km), followed by Adventure Rupes ($\sim$1.3 km) and Resolution Rupes ($\sim$0.9 km) (Figs. 3–6). Discovery Rupes also has the greatest length ($\sim$550 km), followed by Adventure ($\sim$270 km) and Resolution Rupes ($\sim$190 km). Profiles across Discovery, Resolution, and Adventure Rupes show that the vergent side of the structures (the scarp faces) occur on the convex side of the arc (Figs. 4–6). This suggests that the thrust faults dip to the concave side of the arc formed by the lobate scarps.

The strong arcuate trend of Adventure and Resolution Rupes suggests that they are two segments of a single structure (Figs. 1 and 2). Based on an analysis of stereoimages, Dzurisin (1978) suggested that the two structures are topographically continuous. Our DEM shows that the topographic expression of the scarp face of the two structures is continuous except where it is interrupted by the presence of a prominent high-relief ridge that appears to crosscut the Adventure–Resolution Rupes trend (Figs. 2 and 3). The ridge, (here informally named Rabelais Dorsum, after a nearby crater), not readily apparent in monoscopic Mariner 10 images, but was described by Dzurisin (1978). The northern segment of the Rabelais Dorsum has a maximum relief of $\sim$1.4 km, comparable to that of Discovery Rupes, and extends for $\sim$325 km. Features on the eastern side of Rabelais Dorsum, described by Malin (1977) as lobate fronts, are superimposed on intercrater plains and the walls and floors of a number of craters with no evidence of significant offset. Thus, it is not likely that these features are fault scarps. Malin (1977) suggested that they were formed through mass movement associated with seismic activity or tectonically controlled volcanic extrusion. The morphology of the southern, southwest trending segment of the structure transitions from a high-relief ridge to a lobate scarp (Figs. 2 and 3). The lobate scarp segment is over 140 km in length and offsets the walls and floor material of a crater (72°S, 47°W) (Fig. 2). The transition from a high-relief ridge to a lobate scarp suggests that the origin of the two structures may be related. If the formation of both structures involves reverse faulting, one possible explanation for the contrast in morphology is the dip of the fault plane. High-relief

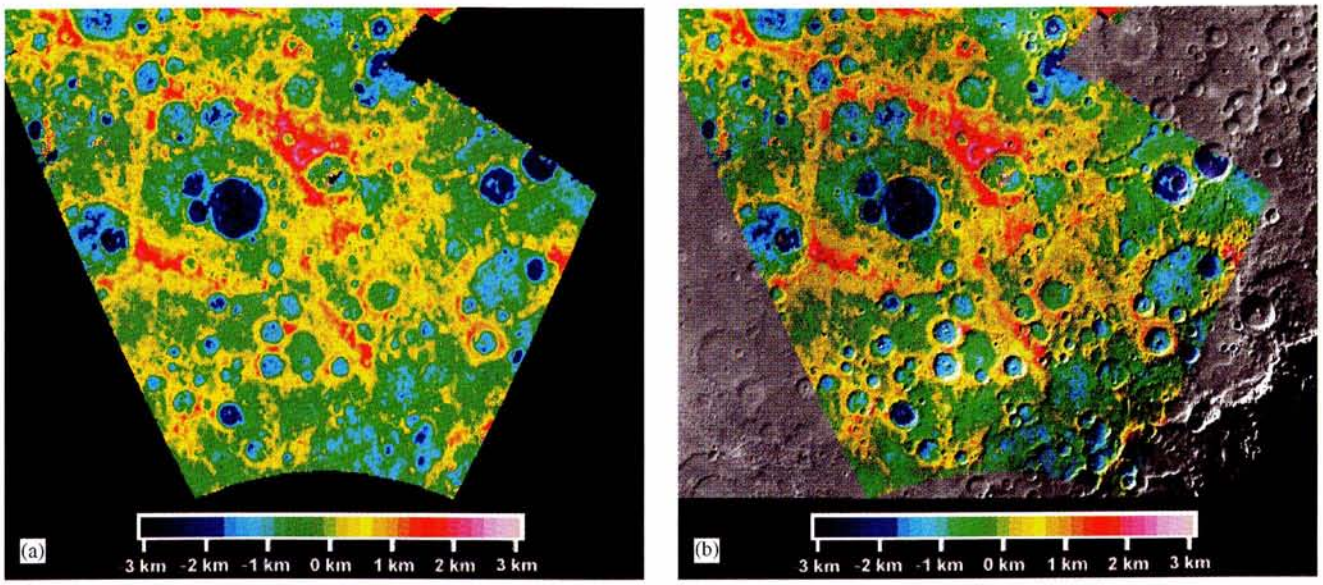

Fig. 3. (a) Regional-scale DEM in the Discovery Rupes region. The DEM mosaic covers the area from 25°W to 80°W, 50°S to 75°S and is a subsection of a larger mosaic (see Fig. 8). (b) Regional-scale DEM overlaid on the photomosaic shown in Fig. 2(a). Shades of cyan to dark blue are lows, and shades of red to pink are highs. Elevations are relative to the 2439.0 km Mercury radius reference sphere.

ridges may reflect deformation over high-angle reverse faults ($\theta > 45^{\circ}$) rather than thrust faults ($\theta < 45^{\circ}$). If this is the case, the change in morphology may reflect the transition from a high-angle reverse fault controlling the northern segment to a thrust fault controlling the southern segment. The morphology and dimension of the high-relief ridge segment of Rabelais Dorsum is similar to high-relief ridges observed in highland material on Mars (Watters, 1993, Fig. 4a). The crosscutting relationship between Rabelais Dorsum and Adventure and Resolution Rupes suggests that the ridge postdates the formation of the thrust fault scarp(s). Rabelais Dorsum, like Adventure and Resolution Rupes, deforms intercrater plains and is superposed by some impact craters. This suggests that the ridge may not be significantly younger than Adventure and Resolution Rupes. The superposition of Rabelais Dorsum on Adventure and Resolution Rupes may indicate a local change in the orientation of the stress field over time.

Another line of evidence that supports the interpretation that Adventure and Resolution Rupes are segments of a single structure is the D–L relationship of the associated thrust faults. The ratio of maximum displacement to fault length γ for the Adventure and Resolution Rupes thrust faults are both $\sim 1.2 \times 10^{-2}$, where the displacement is given by $D = h/\sin\theta$ with h being the measured relief of the scarp and θ the dip of the fault-plane (see Watters et al., 2000). These are almost a factor of 2 higher than γ for other Mercurian thrust faults ($6.5 \pm 3.2 \times 10^{-3}, n = 10$) using estimates of D based on $\theta = 25^{\circ}$ (Watters et al., 2000). If Adventure and Resolution Rupes were formed by a single thrust fault, the fault has a value of γ of $\sim 6.3 \times 10^{-3}$, consistent with that of the Discovery Rupes thrust fault and other Mercurian thrust faults. Thus the orientation, topography, and the D–L relationship all suggest that Adventure and Resolution Rupes are part of the same structure. If this is the case, the Adventure–Resolution Rupes thrust fault is comparable in scale to the Discovery Rupes thrust fault with lengths of $\sim$500 and $\sim$550 km, respectively.

3. Discussion

3.1. Origin of compressional stresses

The origin of compressional stresses that formed the Mercurian thrust faults is thought to have resulted from either global contraction due to secular cooling of the interior, tidal despinning, or a combination of the two (Strom et al., 1975; Cordell and Strom, 1977; Melosh and Dzurisin, 1978; Pechmann and Melosh, 1979; Melosh and McKinnon, 1988). Tidal despinning induces stress into the lithosphere from the relaxation of the equatorial bulge (Melosh and Dzurisin, 1978; Pechmann and Melosh, 1979; Melosh and McKinnon, 1988) and would result in the predominance of E–W compression and thus N–S trending thrust faults. A limitation of the tidal despinning model is that it predicts a system of normal faults at Mercury's poles that have not been observed (see Solomon, 1978; Schubert et al., 1988; Melosh and McKinnon, 1988). During global contraction due to cooling of the interior, the lithosphere is subject to significant thermal stresses (Solomon, 1976, 1978). These stresses

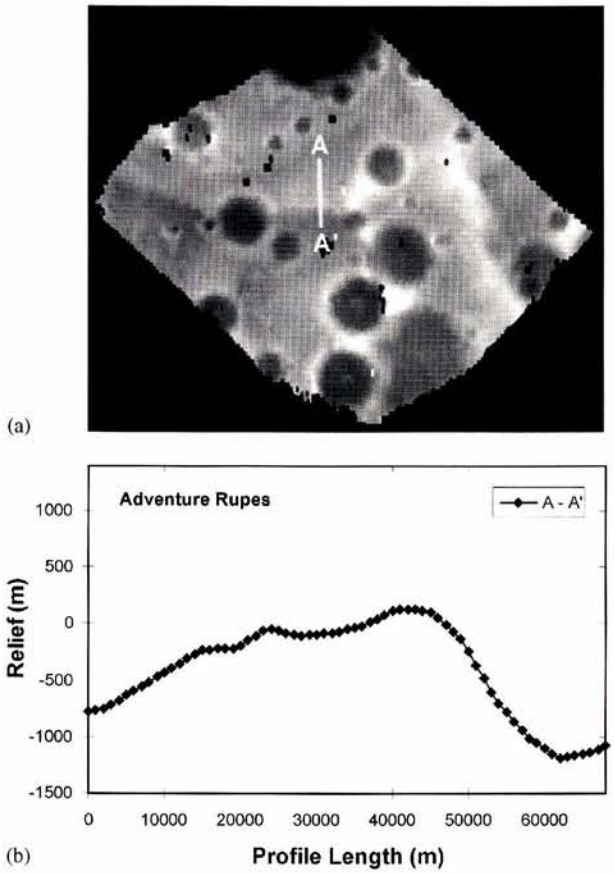

Fig. 4. (a) Digital elevation model of Adventure Rupes generated using the Mariner 10 stereopair. (b) Profile across Adventure Rupes (location is shown in (a)). Elevations are relative to the 2439.0 km Mercury radius reference sphere (vertical exaggeration is ~15:1).

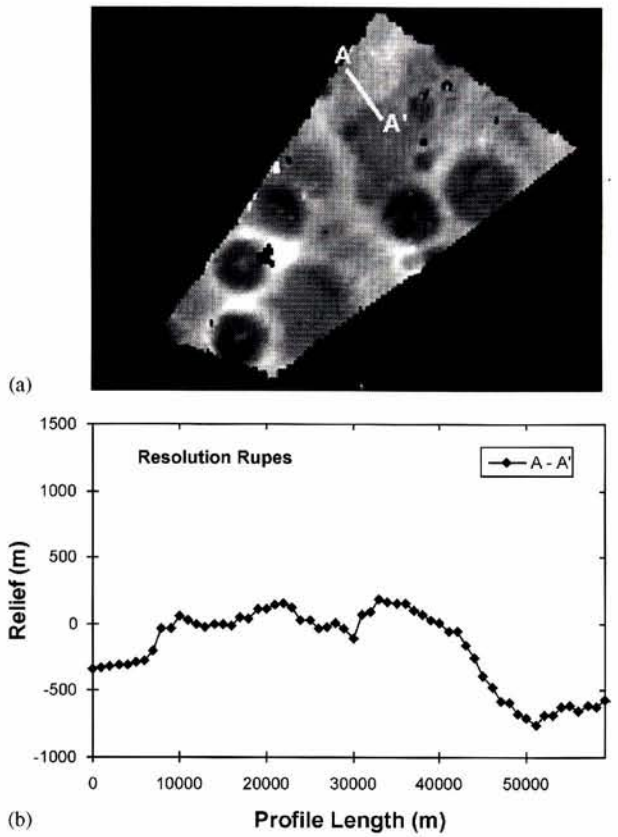

Fig. 5. (a) Digital elevation model of Resolution Rupes generated using the Mariner 10 stereopair. (b) Profile across Resolution Rupes (location is shown in (a)). Elevations are relative to the 2439.0 km Mercury radius reference sphere (vertical exaggeration is ~15:1).

are compressional and horizontally isotropic. The resulting tectonic features would be expected to occur in random patterns (see Janes and Melosh, 1990) with no preferred orientation. The geometry of the thrust faults would also be expected to be random (i.e., no preferred dip direction). The generally distributed nature and random orientations of the Mercurian thrust faults is consistent with this model. Thus at present, the best working model for the origin of lobate scarps is global contraction (Strom et al., 1975; Cordell and Strom, 1977; Phillips and Solomon, 1997; Watters et al., 1998). The distribution, orientation, and inferred geometry of the thrust faults associated with Adventure, Resolution, and Discovery Rupes, however, do not appear to be random. This suggests that the formation of these structures was influenced by regional stresses or by preexisting mechanical discontinuities in the Mercurian crust.

3.2. *Analysis of inferred stresses*

In effort to determine the geometry of the compressional stresses that formed Discovery, Resolution, and Adventure Rupes, an analysis of inferred stresses was performed. The pattern of inferred stresses are examined by fitting great circles, representing traces along the surface of a principal stress trajectory, to each segment and plotting them on an equal-area projection or Schmidt net that represents a hemisphere of the planet (see Wise et al., 1979; Watters, 1993). The direction of the principal stresses are inferred from the orientation of the structure. For the lobate scarps, the maximum compressional stress (σ_1) is assumed to be horizontal and normal to the trace of the thrust faults. The number of intersections is given by $\alpha = n(n-1)/2$ where n is the number of great circles plotted. A perfect radially symmetric system results in a concentration of intersections near 100% per 1% area of the net. Randomly generated points will yield randomly distributed concentrations that decrease in significance with increasing sample size. The orientation of Adventure, Resolution, and Discovery Rupes was approximated by 21 digitized segments. The analysis indicates a maximum concentration of 27% per 1% area ($\alpha = 210$) located at approximately 48°S, 58°W (Fig. 7). The distribution of intersections, however, is not strongly concentric to the point

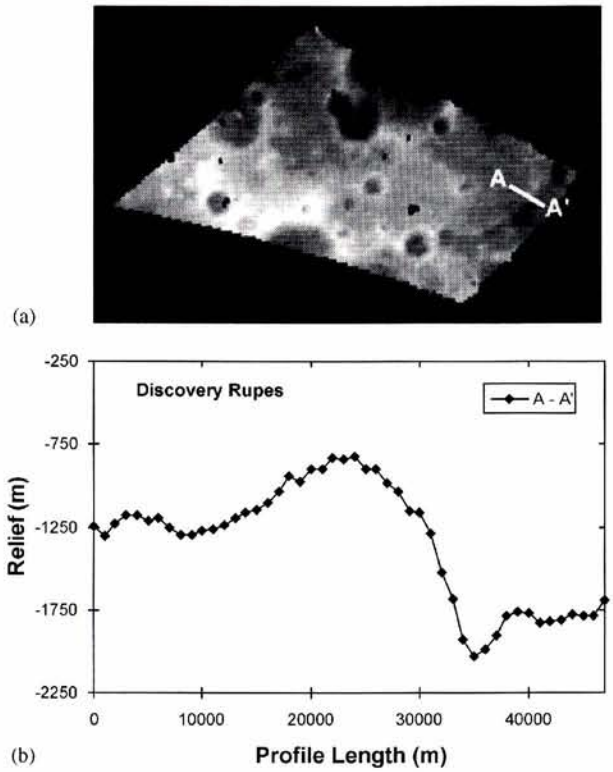

Fig. 6. (a) Digital elevation model of Discovery Rupes generated using the Mariner 10 stereopair. (b) Profile across Discovery Rupes (location is shown in (a)). Elevations are relative to the 2439.0 km Mercury radius reference sphere (vertical exaggeration is ~15:1).

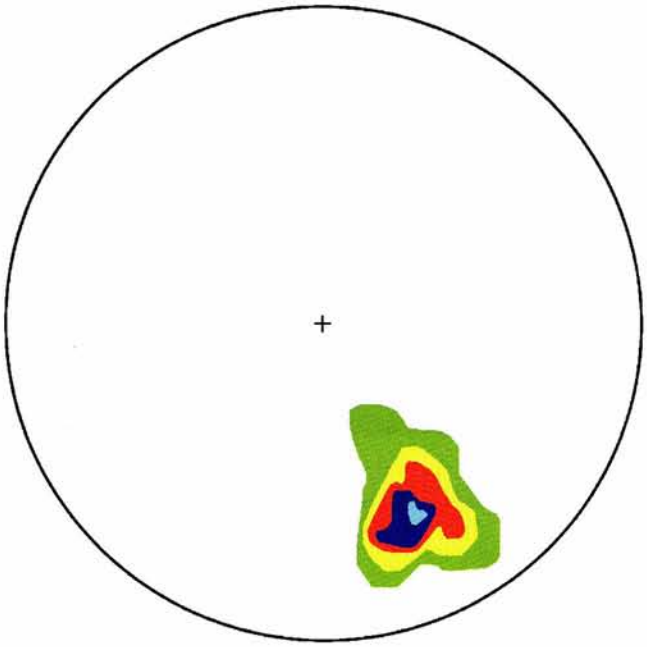

Fig. 7. Equal-area projection showing the concentration of intersections of great circles fit to the inferred maximum principal stress direction of segments of Adventure, Resolution, and Discovery Rupes. Contours indicate 5%, 10%, 15%, 20%, and 25% per 1% area with a maximum density of 27% located at approximately 48°S, 58°W (number of great circles plotted $n = 21$, and the number of intersections $\alpha = 210$). Plot represents the western hemisphere of Mercury and is centered on 0°N, 90°W.

of maximum concentration. It is broad and bimodal indicating that the great circles are radial to two areas in the same region of the Discovery quadrangle.

3.3. *Influence of ancient impact basins*

The results of this analysis are consistent with the hypothesis that the formation of the thrust faults associated with Discovery, Resolution, and Adventure Rupes were influenced by either regional stresses or preexisting mechanical discontinuities in the crust. If global contraction was the predominate source of compressional stress, inhomogeneities in the stress field that allowed a sufficient difference between the horizontal components for one to be maximum are required. However, these conditions would have to have existed over a large area. The lobate scarps may have formed in response to regional compressional stresses; however, there are no obvious sources. Examination of the topography in the area of the maximum concentration of intersections indicates the presence of a broad, shallow, roughly circular depression (Fig. 8). If the thrust faults were localized by a preexisting mechanical discontinuity in the crust, the most plausible source is a buried impact basin.

Spudis and Guest (1988) mapped 20 pre-Tolstojan multiring basins randomly distributed over the Mercurian hemisphere imaged by Mariner 10 on the basis of remnant massifs and circular or arcuate patterns of tectonic features (Pike and Spudis, 1987; Spudis and Guest, 1988). Spudis and Guest (1988) suggest that the population of pre-Tolstojan basins form a structural framework that influenced the subsequent geologic evolution of the surface. The broad, roughly circular, topographic low revealed in the topographic data may be the evidence of another ancient, pre-Tolstojan impact basin, informally named the Bramante–Schubert basin (~550 km in diameter and centered at approximately 43°S, 54°W, Figs. 8 and 9). Segments of Discovery Rupes are roughly concentric to the Bramante–Schubert basin. This may indicate the presence of a ring of the basin that coincides with Discovery Rupes (Fig. 9). Another ring of the Bramante–Schubert basin may coincide with two other lobate scarps in the region, Astrolabe Rupes and Mirni Rupes (Fig. 9). However, segments of Adventure and Resolution Rupes are not strongly concentric to the proposed Bramante–Schubert basin. If the Adventure–Resolution thrust fault was localized by a single basin rim or ring, its presence is not suggested by the topography but rather the arcuate nature of the structure (Fig. 9). It is possible that mechanical discontinuities introduced by ancient buried multiring impact basins influenced the localiza-

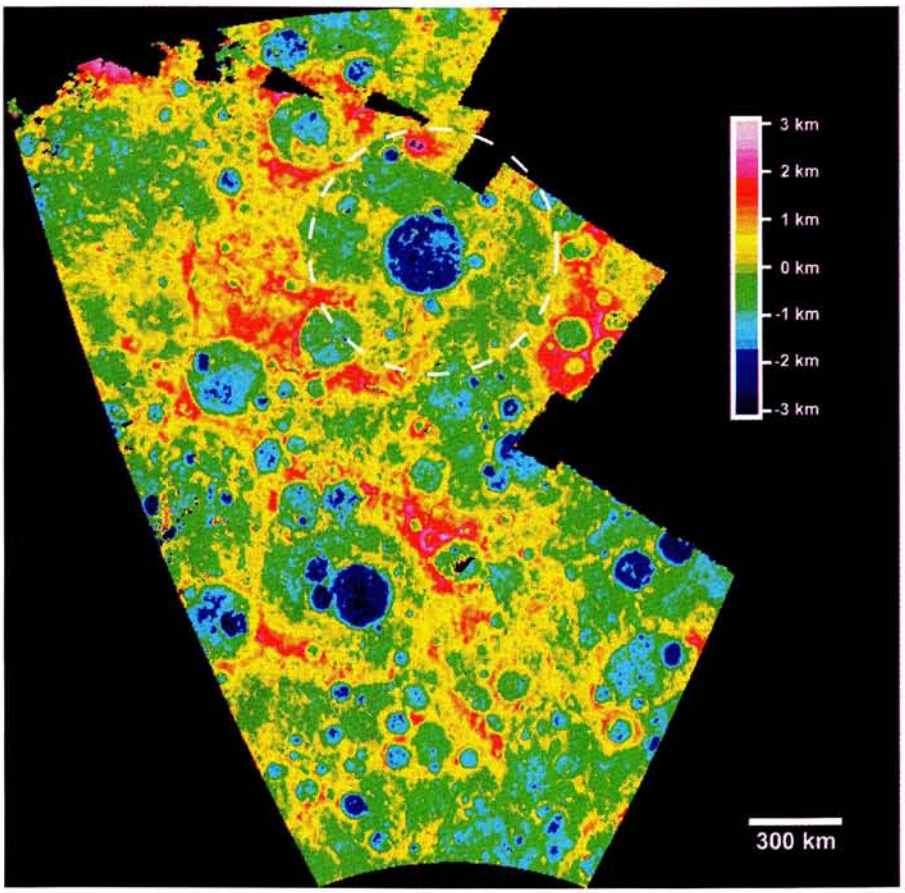

Fig. 8. Regional-scale DEM of part of the Discovery quadrangle. Dashed lines show the proposed location of an ancient impact basin. The DEM covers an area from 25°W to 80°W, 30°S to 75°S and was generated using over 350 individual stereopairs. Shades of cyan to dark blue are lows, and shades of red to pink are highs. Elevations are relative to the 2439.0 km Mercury radius reference sphere.

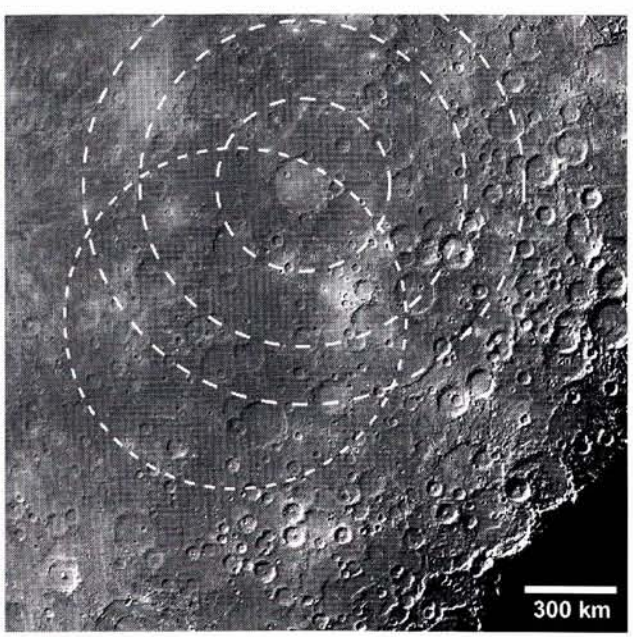

tion of thrust faults forming Adventure, Resolution, and Discovery Rupes. If this is the case, the Adventure–Resolution and Discovery Rupes thrust faults may reflect mechanical discontinuities in the Mercurian crust that are part of a structural framework formed by ancient multiring impact basins as suggested by Spudis and Guest (1988). Such discontinuities in the crust would explain the locally preferred orientation and consistent fault geometry of these thrust faults, formed in response to horizontally isotropic compressional stresses due to global contraction.

Fig. 9. Mariner 10 mosaic showing the proposed location of an ancient, pre-Tolstojan impact basin (lines with long dashes), informally named as Bramante–Schubert basin. The center of the basin (43°S, 54°W) is near the center of Schubert crater. Possible rings of the Bramante–Schubert basin were drawn to coincide with Discovery Rupes (second ring) and Astrolabe and Mirni Rupes (first ring). A possible ring from an unidentified basin was drawn to coincide with the arcuate trend of Adventure and Resolution Rupes (line with small dashes). The same area is shown in Fig. 1.

Thermal history models for Mercury predict gradual cooling of the interior through conduction (Solomon, 1976, 1977, 1979) and mantle convection (Schubert et al., 1988). Thus compressional stresses due to global contraction persisted over a long period in the geologic history of the planet. This is reflected by the presence of lobate scarps in units as old as the intercrater plains and as young as smooth plains (Strom et al., 1975; Melosh and McKinnon, 1988). The formation of the Adventure–Resolution and Discovery Rupes thrust faults and other thrust faults in the intercrater plains suggests the most intense period of deformation initiated after the period of heavy bombardment, before the emplacement of younger plains units.

Acknowledgements

We thank Sean C. Solomon and Paul D. Spudis for their reviews of the manuscript. This research was supported by grants from National Aeronautics and Space Administration's Planetary Geology and Geophysics Program.

References

Cook, A.C., Robinson, M.S., 2000. Mariner 10 stereo image coverage of Mercury. J. Geophys. Res. 105, 9429–9443.

Cordell, B.M., Strom, R.G., 1977. Global tectonics of Mercury and the Moon. Phys. Earth Planet. Inter. 15, 146–155.

Cowie, P.A., Scholz, C.H., 1992. Displacement–length scaling relationship for faults: data synthesis and discussion. J. Struct. Geol. 14, 1149–1156.

Day, T., Cook, A.C., Muller, J.P., 1992. Automated digital topographic mapping techniques for Mars. Int. Arch. Photogramm. Remote Sensing 29, 801–808.

Dzurisin, D., 1978. The tectonic and volcanic history of Mercury as inferred from studies of scarps, ridges, troughs, and other lineaments. J. Geophys. Res. 83, 4883–4906.

Hapke, B., Danielson, E., Klaasen, K., Wilson, L., 1975. Photometic observations of Mercury from Mariner 10. J. Geophys. Res. 80, 2431–2443.

Harmon, J.K., Campbell, D.B., Bindschadler, D.L., Head, J.W., Shapiro, I.I., 1986. Radar altimetry of Mercury: a preliminary analysis. J. Geophys. Res. 91, 385–401.

Harmon, J.K., Campbell, D.B., 1988. Radar observations of Mercury. In: Vilas, F., Chapman, C.R., Matthews, M.S. (Eds.), Mercury. The University of Arizona Press, Tucson, AZ.

Janes, D.M., Melosh, H.J., 1990. Tectonics of planetary loading: a general model and results. J. Geophy. Res. 95, 21,345–21,355.

Malin, M.C., 1977. Observations of intercrater plains on Mercury. Geophys. Res. Lett. 3, 581–584.

Malin, M.C., Dzurisin, D., 1976. Landform degradation on Mercury, the Moon, and Mars: evidence form crater depth/diameter relationships. J. Geophys. Res. 82, 376–388.

Melosh, H.J., Dzurisin, D., 1978. Mercurian global tectonics: a consequence of tidal despinning?. Icarus 35, 227–236.

Melosh, H.J., McKinnon, W.B., 1988. The tectonics of Mercury. In: Vilas, F., Chapman, C.R., Matthews, M.S. (Eds.), Mercury. The University of Arizona Press, Tucson, AZ.

Mouginis-Mark, P.J., Wilson, L., 1981. MERC: a FORTRAN IV program for the production of topographic data for the planet Mercury. Comput. Geosci. 7, 35–45.

Pechmann, J.B., Melosh, H.J., 1979. Global fracture patterns of a despun planet: application to Mercury. Icarus 38, 243–250.

Phillips, R.J., Solomon, S.C., 1997. Compressional strain history of Mercury (abstract). Proceedings of the 28th Lunar and Planetary Science Conference, pp. 1107–1108.

Pike, R.J., 1988. Geomorphology of impact craters on Mercury. In: Vilas, F., Chapman, C.R., Matthews, M.S. (Eds.), Mercury. The University of Arizona Press, Tucson, AZ.

Pike, R.J., Spudis, P.D., 1987. Basin-ring spacing on the Moon, Mercury, and Mars. Earth Moon Planets 39, 129–194.

Robinson, M.S., Lucey, P.G., 1997. Recalibrated Mariner 10 color mosaics: implications for mercurian volcanism. Science 275, 197–200.

Robinson, M.S., Davies, M.E., Colvin, T.R., Edwards, K.E., 1999. A revised control network for Mercury. J. Geophys. Res. 104, 30,847–30,852.

Schenk, P., Melosh, H.J., 1994. Lobate thrust scarps and the thickness of Mercury's lithosphere (abstract). Proceedings of the 25th Lunar and Planetary Science Conference, pp. 1203–1204.

Schubert, G., Ross, M.N., Stevenson, D.J., Spohn, T., 1988. Mercury's thermal history and the generation of its magnetic field. In: Vilas, F., Chapman, C.R., Matthews, M.S. (Eds.), Mercury. The University of Arizona Press, Tucson, AZ.

Solomon, S.C., 1976. Some aspects of core formation in Mercury. Icarus 28, 509–521.

Solomon, S.C., 1977. The relationship between crustal tectonics and internal evolution in the Moon and Mercury. Phys. Earth Planet. Inter. 15, 135–145.

Solomon, S.C., 1978. On volcanism and thermal tectonics on one-plate planets. Geophys. Res. Lett. 5, 461–464.

Solomon, S.C., 1979. Formation, history and energetics of cores in the terrestrial planets. Phys. Earth Planet. Inter. 19, 168–182.

Spudis, P.D., Guest, J.E., 1988. Stratigraphy and geologic history of Mercury. In: Vilas, F., Chapman, C.R., Matthews, M.S. (Eds.), Mercury. The University of Arizona Press, Tucson, AZ.

Strom, R.G., Trask, N.J., Guest, J.E., 1975. Tectonism and volcanism on Mercury. J. Geophys. Res. 80, 2478–2507.

Thomas, P.G., Masson, P., Fleitout, L., 1988. Tectonic history of Mercury. In: Vilas, F., Chapman, C.R., Matthews, M.S. (Eds.), Mercury. The University of Arizona Press, Tucson, AZ.

Thornhill, G.D., Rothery, D.A., Murray, J.B., Cook, A.C., Day, T., Muller, J.P., Iliffe, J.C., 1993. Topography of Apollinaris Patera and Ma'adim Vallis: automated extraction of digital elevation models. J. Geophys. Res. 98, 23,581–23,587.

Watters, T.R., 1993. Compressional tectonism on Mars. J. Geophys. Res. 98, 17,049–17,060.

Watters, T.R., Robinson, M.S., Cook, A.C., 1998. Topography of lobate scarps on Mercury: new constraints on the planet's contraction. Geology 26, 991–994.

Watters, T.R., Robinson, M.S., 1999. Lobate scarps and the Martian crustal dichotomy. J. Geophys. Res. 104, 18,981–18,900.

Watters, T.R., Robinson, M.S., Schultz, R.A., 2000. Displacement–length relations of thrust faults associated with lobate scarps on Mercury and Mars: comparison with terrestrial faults. Geophys. Res. Lett. 27, 3659–3662.

Wise, D.U., Golombek, M.P., McGill, G.E., 1979. Thrasis province of Mars: geologic sequence, geometry and a deformation mechanism. Icarus 38, 456–472.